

Catalytic Graphitization of Cellulose Using Nickel as Catalyst

Chao Chen,^{a,c} Kang Sun,^{a,b,c} Ao Wang,^a Siqun Wang,^c and Jianchun Jiang^{a,b,*}

Microcrystalline cellulose was pyrolyzed and catalytically graphitized under temperatures ranging from 1000 °C to 1600 °C in the presence of nickel (Ni). Optimal conditions for graphitization were determined, along with the structure and conductivity of the resulting samples. The optimal conditions were identified as heating at 1400 °C for 3 h with 3 mmol Ni loading per gram of carbon. The samples obtained had excellent graphitic crystallinity comparable to that of commercial graphite. However, in the absence of Ni loading, no obvious graphitic structure appeared after heating under the same conditions, indicating that Ni was an efficient catalyst for the graphitization of cellulose-based carbon. High-resolution transparent electron microscopy (HRTEM) images showed well-defined graphitic structures of more than 30 layers with slice gaps of 0.340 nm. The conductivities of the samples treated under different temperatures varied from 27 S·cm⁻¹ to 54 S·cm⁻¹ under 20 MPa of pressure, and higher temperatures led to higher conductivity due to better graphitic crystallinity. This study fills an important area of research on the catalytic graphitization of cellulose and provides a reference for the preparation of other cellulose-based graphitic materials.

Keywords: Catalytic graphitization; Cellulose; Nickel; Conductivity

Contact information: a: Research Institute of Forestry New Technology, Chinese Academy of Forestry (CAF), Xiangshan Road, Beijing, 100091, China; b: Institute of Chemical Industry of Forest Products, CAF; National Engineering Laboratory for Biomass Chemical Utilization; Key and Open Lab of Forest Chemical Engineering, SFA; Key Laboratory of Biomass Energy and Material, Jiangsu Province; Nanjing 210042, China; c: Center for Renewable Carbon, University of Tennessee, 2506 Jacob Drive, 37996, Tennessee, USA; *Corresponding author: biomass2016@163.com

INTRODUCTION

Graphite is the most stable form of carbon under standard conditions. It possesses excellent thermal stability and electric conductivity, which have led to its widespread application in such varied areas as electrode materials, refractory materials, and steelmaking (Takeuchi *et al.* 2014). Besides, graphite is considered to be an ideal precursor for the production of few-layered graphene sheets, which have attracted increasing interest in recent years (Castarlenas *et al.* 2014; Amiri *et al.* 2017). However, natural graphite is not a renewable resource. Thus, some kinds of materials, such as petroleum coke or pitch that forms graphitizable carbon precursor after heating, are commonly utilized for the preparation of graphite. Under extremely high temperatures (always above 2800 °C), the disordered microstructures in the precursors can be transformed into highly ordered graphitic structures. This process increases the energy consumption, the cost, and the complexity (Greene *et al.* 2002; Yoon *et al.* 2005; Fan and Han 2011; Huang *et al.* 2013). As a result, the development of new materials and new graphitization methods for the preparation of graphite or graphitic material is desirable, both to replace the use of scarce natural graphite and to find ways to produce commercial graphite at lower temperatures.

As an inexpensive, cheap, biocompatible, abundant, and renewable natural resource, cellulose is an excellent candidate for the production of graphite (Herring *et al.* 2003; Sevilla and Fuertes 2010; Glatzel *et al.* 2013; Hoekstra *et al.* 2015). Thus,

further production of few-layered graphene from cellulose is valuable and promising. However, its use presents great challenges because cellulose forms non-graphitizing amorphous carbon after carbonization, which means that the obtained highly disordered and anisotropic carbon cannot be effectively graphitized even at 3000 °C, which is the heat required to graphitize petroleum coke or pitch (Franklin 1951; Dahn *et al.* 1995). Therefore, the generally used heating method is not suitable for cellulose. In this case, an alternative method – catalytic graphitization – may be preferable.

Catalytic graphitization utilizing transition metals, such as Fe, Co, Ni, Mn, or metalloid element B (Kawanoa *et al.* 1999; Maldonado-Hódar *et al.* 2000; Sevilla and Fuertes 2006; Wang *et al.* 2011; Al-Falahi 2014; Wang *et al.* 2016), has been widely reported as an effective approach for the structural transformation of graphitizable amorphous carbon obtained from pitch (Zhai *et al.* 2011; Khokhlova *et al.* 2015), petroleum coke (Gumaste *et al.* 2012), or polymers such as phenolic resin or polyacrylonitrile (PAN) (Lu *et al.* 2006; Tzeng 2006; Chen *et al.* 2008; Yi *et al.* 2009; Zhao and Song 2011; Wen *et al.* 2012; Al-Falahi 2014) to obtain clear graphitic structures at temperatures below 1000 °C.

Of the catalysts named above, Ni has been found to be particularly effective and has been generally used to obtain graphitic structures with relatively high crystallinity (Sevilla and Fuertes 2006). Although catalytic graphitization is effective with a number of carbon materials, there has been much less research into the graphitization of cellulose as compared to petroleum coke or pitch, primarily because the structural transformation of cellulose-based non-graphitizable carbon is very difficult even at extremely high temperatures.

Despite the relative lack of research on the subject, there are indications that catalytic graphitization may also be effective for cellulose or high-cellulose-containing materials. For instance, Sevilla and Fuertes prepared graphitic nanostructures with a coil morphology from cellulose-based hydrochar in the presence of Ni at 900 °C (Sevilla and Fuertes 2010). Herring produced well-defined hollow carbon nanospheres with excellent graphitic structure from Ni-doped cellulose that was laser-pyrolyzed at 2250 °C (Herring *et al.* 2003). Hoekstra pyrolyzed microcrystalline cellulose spheres homogeneously loaded with base metal salts (nitrates of nickel, cobalt, and iron) under N₂ atmosphere in the temperature range from 500 to 800 °C, and turbostratic graphitic nanoribbons were formed under such conditions (Hoekstra *et al.* 2015). Liu prepared activated carbon with 3 to 8 ultra-thin graphitic layers using leaves of *Zizania latifolia* as a starting material at 900 °C with the assistance of Ni; in that study, approximately 30 graphitic layers were observed when the heating temperature was increased to 1000 °C (Liu *et al.* 2013).

All of these studies involved the graphitization of cellulose at relatively lower temperatures (900 °C) or extremely high temperatures (2250 °C). However, to date, there is still a lack of research on the graphitization of cellulose at temperatures ranging from 1000 °C to 2000 °C. Taking Liu's report (*ibid.*) into account, it is possible that better graphitic structures may be more likely to be generated at heating temperatures above 1000 °C and that therefore, an appropriate temperature for obtaining the best graphitic structure may exist between 1000 °C and 2000 °C.

For this investigation, the authors studied the catalytic graphitization of cellulose at temperatures ranging from 1000 °C to 1600 °C, and the optimal conditions for such graphitization were determined in detail. Finally, the conductivity of all the products was recorded to further evaluate the graphitic crystallinity of the cellulose-based carbons that were obtained.

EXPERIMENTAL

Materials

Microcrystalline cellulose (Aladdin Co., Ltd., Shanghai, China) with an average diameter of 50 μm was put in a quartz boat and carbonized under a nitrogen atmosphere at 500 $^{\circ}\text{C}$ for 1 h. The obtained carbon with a yield of about 28%, was impregnated overnight with nickel chloride (NiCl_2) solution at 0.5 mmol/g to 5 mmol/g Ni to carbon. The impregnated samples were dehydrated at 120 $^{\circ}\text{C}$ and then calcined in sealed crucibles at temperatures ranging from 1000 $^{\circ}\text{C}$ to 1600 $^{\circ}\text{C}$ for 3 h, during which time the catalytic graphitization reaction occurred. For preventing the oxidation during graphitization, the dried samples were put on the bottom of the crucibles, and then covered with granular coconut shell carbon until the crucibles were full. The coconut shell carbon that was present consumed the majority of oxygen, maintaining a reductive atmosphere for graphitization and leading to a relatively high final yield (after removing Ni), *i.e.* 72%, 66%, and 49% for the samples heated at 1000 $^{\circ}\text{C}$, 1400 $^{\circ}\text{C}$, and 1600 $^{\circ}\text{C}$, respectively. After heating, all of the samples were cooled to room temperature, and then they were separated from coconut shell carbon through a sieve. The powder samples were washed with HCl (37%) to remove the metal residue and finally dehydrated at 105 $^{\circ}\text{C}$ overnight. The control sample was prepared in the same process at 1600 $^{\circ}\text{C}$, but without the addition of Ni. For convenience, the obtained samples were denoted as C-X-Y (C representing cellulose, and X and Y representing temperature and Ni loading amount, respectively).

Methods

The X-ray powder diffraction (XRD) patterns for all samples were obtained on a Bruker D8 instrument (Bruker Corporation, Karlsruhe, Germany) operating at 40 kV and 20 mA with Cu $K\alpha$ radiation ($\lambda = 0.15406$ nm) and with measuring angles ranging from 10 $^{\circ}$ to 80 $^{\circ}$. The determination of the graphitized samples and control sample was carried out on a Thermo DXR532 Raman microscope (Thermo Fisher Scientific Inc., Waltham, USA) in the range of 50 cm^{-1} to 3500 cm^{-1} . X-ray photoelectron microscopy (XPS) spectra were recorded on a Kratos Axis Ultra DLD spectrometer (Kratos Analytical Co., Ltd., Manchester, UK). For observation of their morphology, the graphitized samples were first well dispersed in alcohol and treated with an ultrasonic processor followed by coating to copper grids. The coated grids were placed into a JEM2100 transparent electron microscope (Japan Electron Optics Laboratory Co., Ltd., Tokyo, Japan) operated at 200 kV accelerating voltage. The conductivity of all graphitized samples was determined on a ST2722SD powder resistivity instrument (Suzhou Jing-Ge Electronic Co., Ltd., Suzhou, China) under pressures varying from 2 MPa to 20 MPa.

RESULTS AND DISCUSSION

XRD Patterns Utilized for Condition Optimization

To ensure the optimal conditions for graphitization, the two most likely factors, heating temperature and nickel loading amount, were evaluated. First, the influence of temperature was determined by XRD, as shown in Fig. 1(a) with a Ni loading amount 3 mmol/g referring to previous reports. The strong, sharp peak at around 26 $^{\circ}$ (C002), which was widely utilized to determine the degree of graphitization (Pudukudy *et al.* 2016), indicated that obvious graphitization occurred after the heating temperature reached 1000 $^{\circ}\text{C}$; the higher the heating temperature, the stronger the peaks were at heating temperatures ranging from 1000 $^{\circ}\text{C}$ to 1400 $^{\circ}\text{C}$. At heating temperatures

higher than 1400 °C, the graphitic crystallinity of the samples no longer increased, which can be deduced from the fact that Samples C-1400-3 and C-1600-3 had almost the same XRD patterns. Moreover, as can be seen in Fig. 1(b), C-1400-3's characteristic peak had almost the same intensity as that of commercial graphite, indicating the existence of graphitic structures with similarly high crystallinity. It is also notable that the characteristic peaks of all prepared samples slightly shifted to lower 2θ angles (26.2°) than graphite (26.5°), which suggested that the obtained graphitic structure had greater interplanar spacing ($d_{002} = 0.340$ nm) than graphite ($d_{002} = 0.335$ nm), as calculated according to Bragg's equation. As has been reported, the graphitic structures obtained by catalytic graphitization have the same layer spacing as the products in this study (Sevilla *et al.* 2007; Anton 2008). Such structures are similar to graphene sheets or may even be regarded as graphene (Anton 2008; Jiang *et al.* 2010); thus the authors inferred that prepared graphitic structures were more likely to be composed of few layered graphene (Pudukudy *et al.* 2016). Furthermore, it was clearly seen that the control sample heated at 1600 °C without Ni had no clear characteristic peak for graphitic structure, indicating that the carbon remains an amorphous structure in the absence of Ni as a catalyst. Thus, the authors concluded that the optimal temperature for graphitization was 1400 °C, the temperature at which graphitic structures with high crystallinity similar to graphite were obtained.

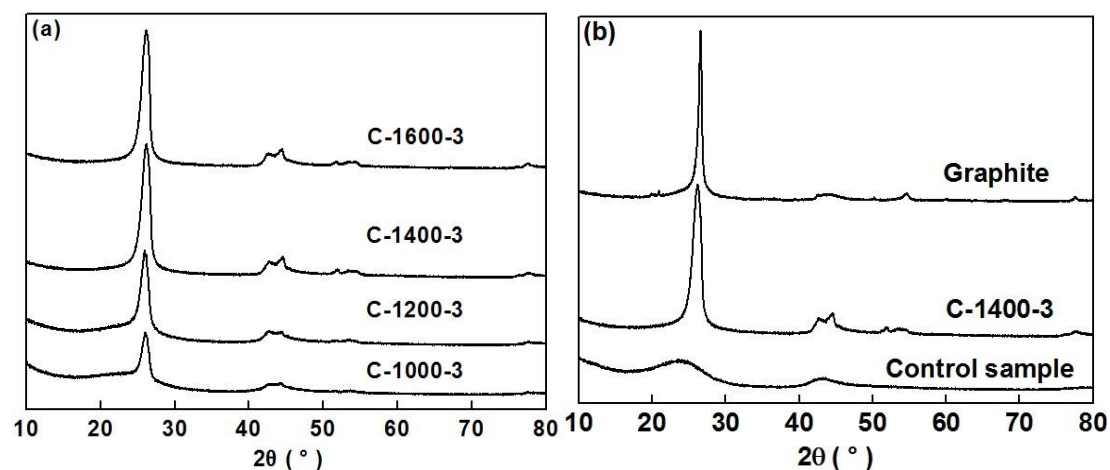


Fig. 1. XRD patterns of cellulose treated with Ni at different temperatures (a), compared with XRD patterns of graphite, C-1400-3, and the control sample (b)

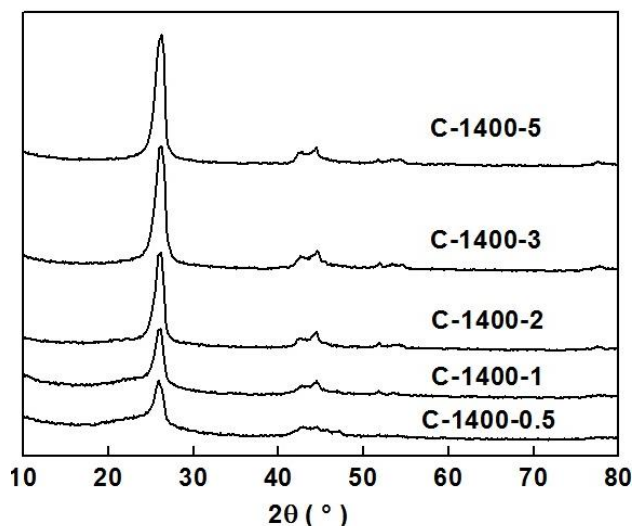


Fig. 2. XRD patterns of samples with different Ni loading amounts

It is known that graphitization occurs only in areas where carbon contacts Ni (Sevilla and Fuertes 2010). So the authors surmised that a higher Ni loading amount might also create more contact areas, resulting in greater graphitization. Thus, the optimal loading amount was determined at 1400 °C by XRD, as shown in Fig. 2. From the clearly increased characteristic peak, it was deduced that the degree of graphitization dramatically increased as catalyst amounts were increased from 0.5 to 3 mmol/g. However, when further loading was added up to 5 mmol/g, the crystallinity barely increased, illustrating that 3 mmol/g was an appropriate loading amount.

Raman, XPS, and TEM analysis

Raman curves for the graphitized sample and the control sample treated without Ni are shown in Fig. 3. It is known that for carbon-based materials, there are two distinct peaks in Raman spectra – the D band at around 1340 cm^{-1} and the G band at around 1570 cm^{-1} , which correspond to diamond-like carbon (sp^3 -bonded) and graphitic carbon (sp^2 -bonded), respectively. The intensity ratios of the D band and the G band (I_D/I_G) are widely used to estimate the degree of graphitization (Sevilla *et al.* 2007), and it is known that a smaller ratio of I_D/I_G produces a better graphitic structure (Liu *et al.* 2004; Pudukudy and Yaakob 2015). It is calculated that the I_D/I_G ratio was approximately 0.5 for the sample C-1400-3, indicating that an obvious graphitic structure appeared with the assistance of Ni, while this ratio for the control sample was approximately 1.2, proving that the control sample remained amorphous carbon structure in the absence of Ni (Zhang *et al.* 2000). Besides, the sharp 2D band lower than G further indicated the existence of few layered graphene sheets (Pudukudy *et al.* 2017).

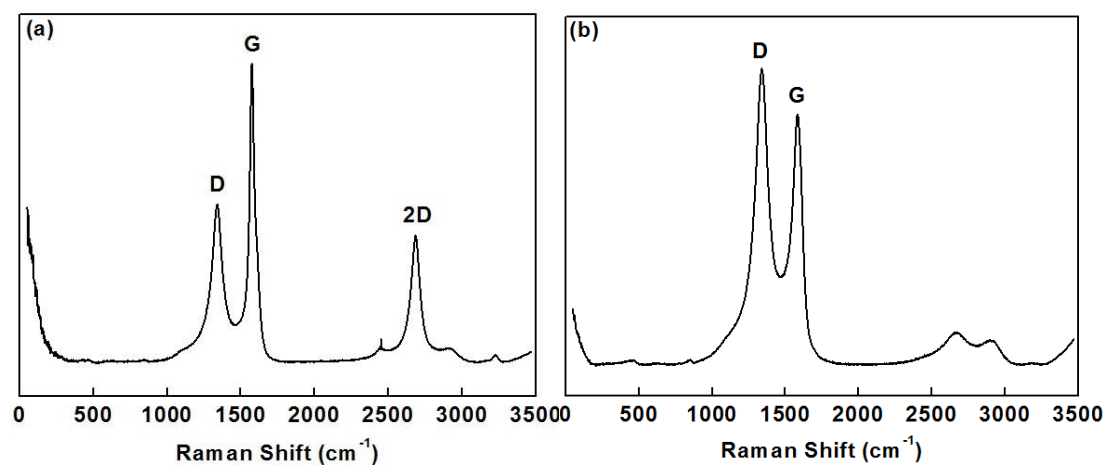


Fig. 3. Raman spectra for C-1400-3 (a) and the control sample (b)

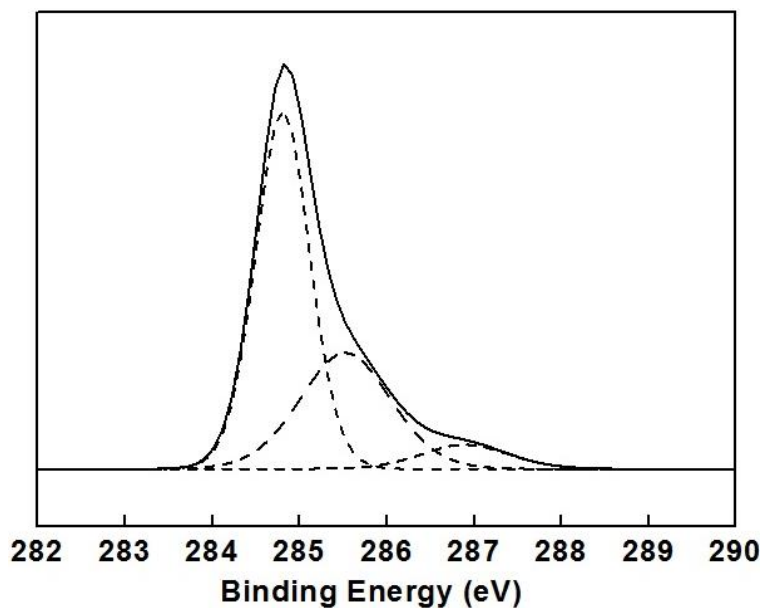


Fig. 4. XPS spectrum for the sample C-1400-3

Figure 4 shows the XPS spectra of C-1400-3. Remarkably, there were three peaks (dotted areas) attributable to three series of carbons: graphitic carbon, *i.e.* C=C groups ($E_B = 284.8$ eV), amorphous carbon, *i.e.* C-C or CH_x groups ($E_B = 285.5$ eV), and carbonyl carbon, *i.e.* C=O groups ($E_B = 286.9$ eV) (Okpalugo *et al.* 2005). From the ratio of corresponding peaks, the graphitic/amorphous ratio was calculated as 1.80. This ratio was much higher than the reported value of 0.756 (Sevilla and Fuertes 2010), indicating the existence of a higher proportion of graphitic carbon in the sample C-1400-3, which was treated at a higher temperature than reported.

A clear structural difference can be seen by comparing Figs. 5(a) and (b): the graphitic sample C-1400-3 showed clear ribbon-like structures composed of 10 to approximately 30 graphitic layers. In contrast, the control sample had no characteristic structure or shape, indicating that there was no reaction leading to obvious structure transformation in the absence of Ni. High-resolution transparent electron microscopy (HRTEM) micrographs of C-1400-3 and the control sample are shown in Figs. 4(c) and (d), respectively.

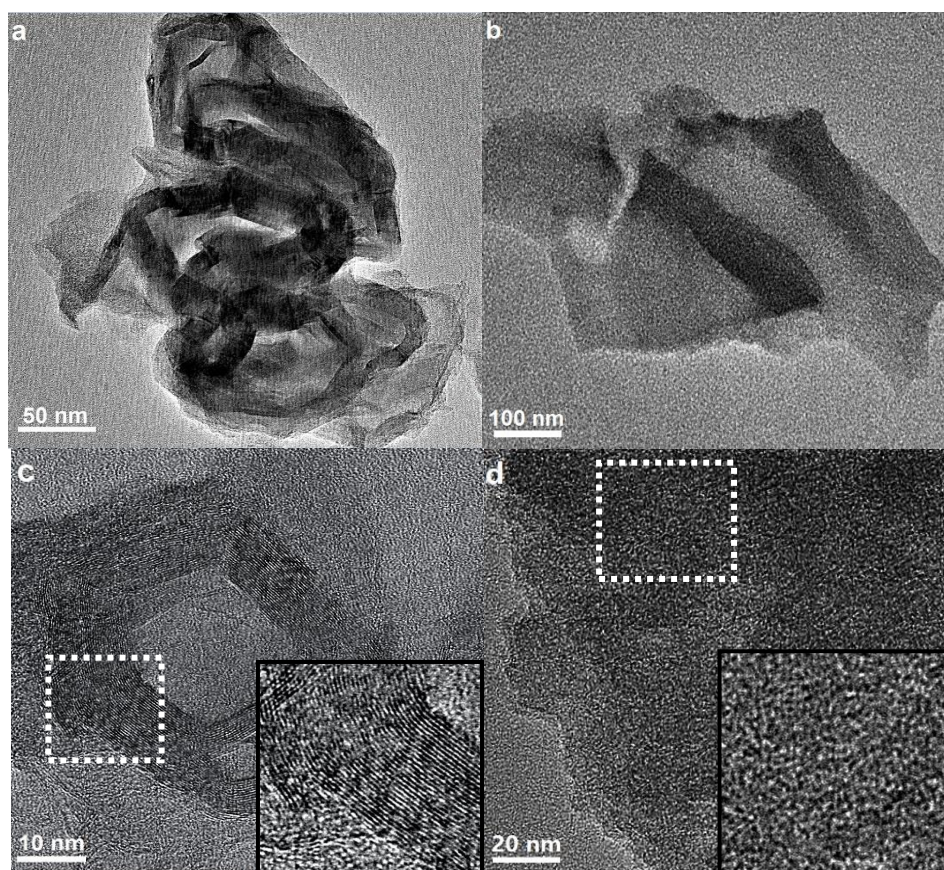


Fig. 5. Low magnification TEM micrographs for C-1400-3 (a); the control sample (b); HRTEM images for C-1400-3 (c); and the control sample (d) (Inset: magnified image of dotted square)

Obvious graphitic structures, or also defined as few layered graphene sheets (Pudukudy *et al.* 2017) in C-1400-3 with more than 30 layers, can be seen in Fig. 5(c), while in the control sample, only short and randomly oriented amorphous carbon structures could be seen (Fig. 5(d)). Interestingly, the obtained graphite layers formed a nearly annular structure rather than a continuously straight structure. Consistent with previous report (Brockner *et al.* 2007), during the high-temperature reaction, the nickel salts, such as NiCl_2 or $\text{Ni}(\text{NO}_3)_2$, first decomposed to form nickel oxide and then were reduced to metallic Ni by reacting with surrounding carbon. The metallic molten-like Ni thus generated continued to react with surrounding amorphous carbon following the well-known “dissolution-precipitation” process, during which amorphous carbon and Ni formed liquid metal-carbon composite particles followed by the release of metal and graphitic carbon (Sevilla and Fuertes 2010; Bokhonov *et al.* 2015). The liquid Ni nanoparticles were able to move, leading to effective graphitization, and higher temperatures spurred the formation of larger Ni nanoparticles, resulting in the generation of more graphitic layers. After the removal of Ni particles, the obtained graphitic structure with annular shape can be seen in the TEM images.

Conductivity Test

Conductivity is another indicator for evaluating the crystallinity of graphitic structure. Higher conductivity implies improved graphitic structure. As illustrated in Fig. 6(a), the conductivities for both C-1400-3 and the control sample increased from $7.3 \text{ S}\cdot\text{cm}^{-1}$ and $12.4 \text{ S}\cdot\text{cm}^{-1}$ to $27.6 \text{ S}\cdot\text{cm}^{-1}$ and $54.5 \text{ S}\cdot\text{cm}^{-1}$, respectively. These increases corresponded to the increase of pressure from 2 MPa to 20 MPa, while the conductivity of the cellulose-based char was too low for detection, indicating that

heating at high temperature benefitted the formation of the graphitic structure. The addition of Ni also enhanced the graphitic crystallinity dramatically, leading to the appearance of the excellent graphitic structure as seen in TEM and the obviously enhanced conductivity. The conductivities of cellulose-based samples treated under different temperatures from 1000 °C to 1600 °C were determined, as shown in Fig. 6(b). Clearly, the higher the heating temperature, the higher the conductivity obtained. In addition, the conductivity increased rapidly when the heating temperature was raised from 1000 °C to 1400 °C, while it increased more slowly at heating temperatures higher than 1400 °C. It was certain that the conductivity corresponded to the graphitic crystallinity, which barely improved at temperatures higher than 1400 °C. Therefore, temperature had the same effect on conductivity as it did on graphitic crystallinity. Although in C-1400-3, the obtained crystallinity was high as that of graphite, the conductivity of the sample was much lower than that of graphite (measured as 685 S·cm⁻¹ at 20 MPa). The same phenomenon has been seen in Sevilla and Fuertes' report, where conductivity was 19.5 S·cm⁻¹ for samples with high graphitic crystallinity catalyzed by Ni (Sevilla and Fuertes 2006). The difference may be attributable to the existence of minority amorphous carbon and the characteristic annular shape, which restricts electron transportation. The authors are currently conducting further research on enhancing conductivity.

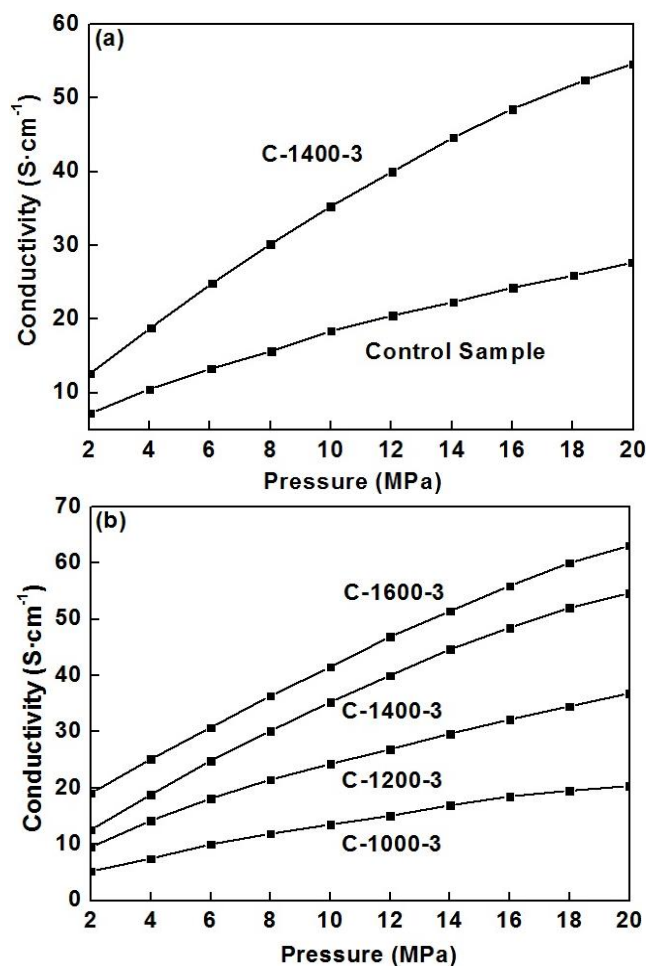


Fig. 6. Comparison of the conductivities of C-1400-3 and the control sample (a) and the conductivities of samples heated at different temperatures (b)

CONCLUSIONS

1. The graphitization of microcrystalline cellulose at temperatures ranging from 1000 °C to 1600 °C was carried out *via* catalytic graphitization in the presence of Ni. The optimal conditions were determined as heating at 1400 °C with a Ni-loading amount of 3 mmol/g for 3 h.
2. The XRD, Raman, and XPS spectra revealed that Sample C-1400-3 had high graphitic crystallinity, similar to graphite, with interplanar spacing of 0.340 nm.
3. The graphitic structure obtained, with more than 30 layers in Sample C-1400-3, showed a clear annular shape due to the dissolution-precipitation mechanism of the reaction that occurred around the metallic Ni particles.
4. The conductivity of the graphitized sample was high at 54.5 S·cm⁻¹ under 20 MPa pressure.
5. This work supplies theoretical guidance for the preparation of cellulose-based graphene in the future.

ACKNOWLEDGMENTS

This work was financially supported by the Fundamental Research Funds of China Academy of Forestry (CAF) (Project No. CAFYBB2014QA024) and the National Natural Science Foundation of China (Project No. 31770629). The authors are grateful for the analytic support of the Instrument Analysis Center and Pulp and Paper Research Lab at the Institute of Chemical Industry of Forest Products, CAF, Nanjing, China.

REFERENCES CITED

- Amiri, A., Zubir, M. N. M., Dimiev, A., M., Teng, K. H., Shanbedi, M., Kazi, S. N., and Rozali, S., B. (2017). "Facile, environmentally friendly, cost effective and scalable production of few-layered graphene," *Chemical Engineering Journal* 326, 1105-1115. DOI: 10.1016/j.cej.2017.06.046
- Al-Falahi, H. A. (2014). "Catalytic graphitization of modified phenolic resin and its nanoparticles fillers behavior towards high temperature," *Advanced Materials Research* 925, 282-289. DOI: 10.4028/www.scientific.net/AMR.925.282
- Anton, R. (2008). "On the reaction kinetics of Ni with amorphous carbon," *Carbon* 46(4), 656-662. DOI: 10.1016/j.carbon.2008.01.021
- Bokhonov, B. B., Dudina, D. V., Ukhina, A. V., Korchagin, M. A., Bulina, N. V., Mali, V. I., and Anisimov, A. G. (2015). "Formation of self-supporting porous graphite structures by spark plasma sintering of nickel–amorphous carbon mixtures," *Journal of Physics and Chemistry of Solids* 76, 192-202. DOI: 10.1016/j.jpics.2014.09.007
- Brockner, W., Ehrhardt, C., and Gjikaj, M. (2007). "Thermal decomposition of nickel nitrate hexahydrate, Ni(NO₃)₂·6H₂O, in comparison to Co(NO₃)₂·6H₂O and Ca(NO₃)₂·4H₂O," *Thermochimica Acta* 456(1), 64-68. DOI: 10.1016/j.tca.2007.01.031
- Castarlenas, S., Rubio, C., Mayoral, A., Téllez, C., and Coronas, J. (2014). "Few-layer graphene by assisted-exfoliation of graphite with layered silicate," *Carbon* 73, 99-105. DOI: 10.1016/j.carbon.2014.02.044
- Chen, K., Wang, C., Ma, D., Huang, W., and Bao, X. (2008). "Graphitic carbon

- nanostructures via a facile microwave-induced solid-state process,” *Chemical Communications* 2008(24), 2765-2767. DOI: 10.1039/B800807H
- Dahn, J. R., Zheng, T., Liu, Y., and Xue, J. S. (1995). “Mechanisms for lithium insertion in carbonaceous materials,” *Science* 270(5236), 590-593. DOI: 10.1126/science.270.5236.590
- Fan, C., and Han, C. (2011). “Preparation, structure, and electrochemical performance of anodes from artificial graphite scrap for lithium ion batteries,” *Journal of Material Science* 46(7), 2140-2147. DOI: 10.1007/s10853-010-5050-y
- Franklin, R. E. (1951). “Crystallite growth in graphitizing and non-graphitizing carbons,” *Proceedings of the Royal Society A* 209(1097), 196-218. DOI: 10.1098/rspa.1951.0197
- Glatzel, S., Schnepf, Z., and Giordano, C. (2013). “From paper to structured carbon electrodes by inkjet printing,” *Angewandte Chemie International Edition* 52(8), 2355-2358. DOI: 10.1002/anie.201207693
- Greene, M., Schwartz, R. E., and Treleaven, J. W. (2002). “Short residence time graphitization of mesophase pitch-based carbon fibers,” *Carbon* 40(8), 1217-1226. DOI: 10.1016/S0008-6223(01)00301-3
- Gumaste, J. L., Mukherjee, P. S., Singh, S. K., and Mishra, B. K. (2012). “Studies on the graphitization of calcined petroleum coke in nitrogen arc plasma,” *International Journal of Science & Technology* 2(3), 85-95.
- Herring, A. M., McKinnon, J. T., McCloskey, B. D., Filley, J., Gneshin, K. W., Pavelka, R. A., Kleebe, H.-J., and Aldrich, D. J. (2003). “A novel method for the templated synthesis of homogeneous samples of hollow carbon nanospheres from cellulose chars,” *Journal of the American Chemical Society* 125(33), 9916-9917. DOI: 10.1021/ja035031j
- Hoekstra, J., Beale, A. M., Soulimani, F., Versluijs-Helder, M., Geus, J. W., and Jenneskens, L. W. (2015). “Base metal catalyzed graphitization of cellulose: A combined Raman spectroscopy, temperature-dependent X-ray diffraction and high-resolution transmission electron microscopy study,” *The Journal of Physical Chemistry C* 119(19), 10653-10661. DOI: 10.1021/acs.jpcc.5b00477.
- Hoekstra, J., Versluijs-Helder, M., Vlietstra, E. J., Geus, J. W., and Jenneskens, L. W. (2015). “Carbon-supported base metal nanoparticles: Cellulose at work,” *ChemSusChem* 8, 985-989. DOI: 10.1002/cssc.201403364.
- Huang, S., Guo, H., Li, X., Wang, Z., Gan, L., Wang, J., and Xiao, W. (2013). “Carbonization and graphitization of pitch applied for anode materials of high power lithium ion batteries,” *Journal of Solid State Electrochemistry* 17(5), 1401-1408. DOI: 10.1007/s10008-013-2003-9
- Jiang, F., Fang, Y., Xue, Q., Chen, L., and Lu, Y. (2010). “Graphene-based carbon nano-fibers grown on thin-sheet sinter-locked Ni-fiber as self-supported electrodes for supercapacitors,” *Materials Letters* 64(2), 199-202. DOI: 10.1016/j.matlet.2009.10.047
- Kawanoa, Y., Fukudaa, T., Kawaradaa, T., Mochidab, I., and Koraib, Y. (1999). “Suppression of puffing during the graphitization of pitch needle coke by boric acid,” *Carbon* 37(4), 555-560. DOI: 10.1016/S0008-6223(98)00221-8
- Khokhlova, G. P., Bamakov, C. N., Malysheva, V. Y., Popova, A. N., and Ismagilov, Z. R. (2015). “Effect of heat treatment conditions on the catalytic graphitization of coal-tar pitch,” *Solid Fuel Chemistry* 49(2), 66-72. DOI: 10.3103/S0361521915020056
- Liu, Y., Liu, Q., Gu, J., Kang, D., Zhou, F., Zhang, W., Wu, Y., and Zhang, D. (2013). “Highly porous graphitic materials prepared by catalytic graphitization,” *Carbon* 64, 132-140. DOI: 10.1016/j.carbon.2013.07.044

- Liu, Y., Pan, C., and Wang, J. (2004). "Raman spectra of carbon nanotubes and nanofibers prepared by ethanol flames," *Journal of Materials Science* 39(3), 1091-1094. DOI: 10.1023/B:JMSC.0000012952.20840.09
- Lu, A.-H., Li, W.-C., Salabas, E.-L., Spliethoff, B., and Schüth, F. (2006). "Low temperature catalytic pyrolysis for the synthesis of high surface area, nanostructured graphitic carbon," *Chemistry of Materials* 18(8), 2086-2094. DOI: 10.1021/cm060135p
- Maldonado-Hódar, F. J., Moreno-Castilla, C., Rivera-Utrilla, J., Hanzawa, Y., and Yamada, Y. (2000). "Catalytic graphitization of carbon aerogels by transition metals," *Langmuir* 16(9), 4367-4373. DOI: 10.1021/la991080r
- Okpalugo, T., Papakonstantinou, P., Murphy, H., McLaughlin, J., and Brown, N. M. D. (2005). "High resolution XPS characterization of chemical functionalised MWCNTs and SWCNTs," *Carbon* 43(1), 153-161. DOI: 10.1016/j.carbon.2004.08.033
- Pudukudy, M., and Yaakob, Z. (2015). "Methane decomposition over Ni, Co and Fe based monometallic catalysts supported on sol gel derived SiO₂ microflakes," *Chemical Engineering Journal* 262, 1009-1021. DOI: 10.1016/j.cej.2014.10.077
- Pudukudy, M., Kadier, A., Yaakob, Z., and Takriff, M. S. (2016). "Non-oxidative thermocatalytic decomposition of methane into CO_x free hydrogen and nanocarbon over unsupported porous NiO and Fe₂O₃ catalysts," *International Journal of Hydrogen Energy* 41(41), 18509-18521. DOI: 10.1016/j.ijhydene.2016.08.160
- Pudukudy, M., Yaakob, Z., and Takriff, M. S. (2016). "Methane decomposition over unsupported mesoporous nickel ferrites: effect of reaction temperature on the catalytic activity and properties of the produced carbon," *RSC Advances* 6(72), 68081-68091. DOI: 10.1039/c6ra14660k
- Pudukudy, M., Yaakob, Z., Dahani, N., Takriff, M. S., and Hassan, N. S. M. (2017). "Production of CO_x free hydrogen and nanocarbon via methane decomposition over unsupported porous nickel and iron catalysts," *Journal of Cluster Science* 28(3), 1579-1594. DOI: 10.1007/s10876-017-1173-5
- Pudukudy, M., Yaakob, Z., and Akmal, Z. S. (2015). "Direct decomposition of methane over SBA-15 supported Ni, Co and Fe based bimetallic catalysts," *Applied Surface Science* 330, 418-430. DOI: 10.1016/j.apsusc.2015.01.032
- Pudukudy, M., Yaakob, Z., Mazuki, M. Z., Takriff, M. S., and Jahaya, S. S. (2017). "One-pot sol-gel synthesis of MgO nanoparticles supported nickel and iron catalysts for undiluted methane decomposition into CO_x free hydrogen and nanocarbon," *Applied Catalysis B: Environmental* 218, 298-316. DOI: 10.1016/j.apcatb.2017.04.070
- Sevilla, M., and Fuertes, A. B. (2006). "Catalytic graphitization of template mesoporous carbons," *Carbon* 44(3), 468-474. DOI: 10.1016/j.carbon.2005.08.019
- Sevilla, M., and Fuertes, A. B. (2010). "Graphitic carbon nanostructures from cellulose," *Chemical Physics Letters* 490(1-3), 63-68. DOI: 10.1016/j.cplett.2010.03.011
- Sevilla, M., Sanchís, C., Valdés-Solís, T., Morallón, E., and Fuertes, A. B. (2007). "Synthesis of graphitic carbon nanostructures from sawdust and their application as electrocatalyst supports," *Journal of Physical Chemistry C* 111(27), 9749-9756. DOI: 10.1021/jp072246x
- Takeuchi, T., Kageyama, H., Nakanishi, K., Ohta, T., Sakuda, A., Sakai, T., Kobayashi, H., Sakaebe, H., Tatsumi, K., and Ogumi, Z. (2014). "Application of graphite–solid electrolyte composite anode in all-solid-state lithium secondary

- battery with Li₂S positive electrode,” *Solid State Ionics* 262, 138-142. DOI: 10.1016/j.ssi.2013.09.046
- Tzeng, S. (2006). “Catalytic graphitization of electroless Ni-P coated PAN-based carbon fibers,” *Carbon* 44(10), 1986-1993. DOI: 10.1016/j.carbon.2006.01.024
- Wang, K., Cao, Y., Wang, X., Kharel, P. R., Gibbons, W., Luo, B., Gu, Z., Fan, Q., and Metzger, L. (2016). “Nickel catalytic graphitized porous carbon as electrode material for high performance supercapacitors,” *Energy* 101, 9-15. DOI: 10.1016/j.energy.2016.01.059
- Wang, Z., Zhang, X., Liu, X., Lv, M., Yang, K., and Meng, J. (2011). “Co-gelation synthesis of porous graphitic carbons with high surface area and their applications,” *Carbon* 49(1), 161-169. DOI: 10.1016/j.carbon.2010.08.056
- Wen, Y., Lu, Y., Xiao, H., and Qin, X. (2012). “Further investigation on boric acid catalytic graphitization of polyacrylonitrile carbon fibers: Mechanism and mechanical properties,” *Materials and Design* 36, 728-734. DOI: 10.1016/j.matdes.2011.11.051
- Yi, S., Wu, C., Fan, Z., Kuang, Y., and Chen, J. (2009). “Catalytic graphitization of PAN-based carbon fibers by spontaneously deposited manganese oxides,” *Transition Metal Chemistry* 34(5), 559-563. DOI: 10.1007/s11243-009-9229-5
- Yoon, S. B., Chai, G. S., Kang, S. K., Yu, J. S., Gierszal, K. P., and Jaroniec, M. (2005). “Graphitized pitch-based carbons with ordered nanopores synthesized by using colloidal crystals as templates,” *Journal of the American Chemical Society* 127(12), 4188-4189. DOI: 10.1021/ja0423466
- Zhang, S., Zeng, X. T., Xie, H., and Hing, P. (2000). “A phenomenological approach for the I_d/I_g ratio and sp³ fraction of magnetron sputtered a-C films,” *Surface and Coatings Technology* 123(2-3), 256-260. DOI: 10.1016/S0257-8972(99)00523-X
- Zhai, D., Du, H., Li, B., Zhu, Y., and Kang, F. (2011). “Porous graphitic carbons prepared by combining chemical activation with catalytic graphitization,” *Carbon* 49(2), 725-729. DOI: 10.1016/j.carbon.2010.09.057
- Zhao, M., and Song, H. (2011). “Catalytic graphitization of phenolic resin,” *Journal of Materials Science & Technology* 27(3), 266-270. DOI: 10.1016/S1005-0302(11)60060-1

Article submitted: September 14, 2017; Peer review completed: January 13, 2018;
Revised version received and accepted: March 6, 2018; Published: March 13, 2018.
DOI: 10.15376/biores.13.2.3165-3176